ELEVENTH EUROPEAN ROTORCRAFT FORUM

Paper No. 66

An Experimental and Analytical Investigation of Isolated Rotor Flap-Lag Stability in Forward Flight

Gopal H. Gaonkar
Dept. of Mechanical Engineering
Florida Atlantic University
Boca Raton, FL 33431-0991
USA

Michael J. McNulty
Aeromechanics Laboratory
U.S. Army Research & Technology Laboratories (AVSCOM)
Moffett Field, CA 94035
USA

J. Nagabhushanam
Dept of Aerospace Engineering
Indian Institute of Science
Bangalore 560 012
India

September 10-13, 1985

London, England

THE CITY UNIVERSITY, LONDON, EC1V OHB, ENGLAND

An Experimental and Analytical Investigation of Isolated Rotor Flap-Lag Stability in Forward Flight

Gopal H. Gaonkar
Florida Atlantic University
Boca Raton, Florida, USA

Michael J. McNulty
U.S. Army Research & Technology Laboratories
Moffett Field, California, USA

J. Nagabhushanam
Indian Institute of Science
Bangalore, India

ABSTRACT

For flap-lag stability of isolated rotors, experimental and analytical investigations are conducted in hover and forward flight on the adequacy of a linear quasisteady aerodynamics theory with dynamic inflow. Forward flight effects on lag regressing mode are emphasized. Accordingly, a soft inplane hingeless rotor with three blades is tested at advance ratios as high as 0.55 and at shaft angles as high as 20°. The 1.62-m model rotor is untrimmed with an essentially unrestricted tilt of the tip path plane, as is typical of tail rotors. In combination with lag natural frequencies, collective pitch settings and flap-lag coupling parameters, the data base comprises nearly 1200 test points (damping and frequency) in forward flight and 200 test points in hover. A small portion of the forward flight data refers to stall. By computerized symbolic manipulation, an analytical model is developed in substall to predict stability margins with mode indentification. It also predicts substall and stall regions to help explain the correlation between theory and data. The correlation shows both the strengths and weaknesses of the data and theory, and promotes further insights into areas in which further study is needed in substall and stall.

NOMENCLATURE

a	Lift curve slope, rad^{-1}
c_d	Profile drag coefficient
N	Number of blades
R	Flap-lag structural coupling parameter
t	Dimensionless time (identical with blade azimuth position of first blade).
α	Angle of attack
α_s	Rotor shaft angle, positive nose down

β_o (ζ_o), β_s (ζ_s) and β_c(ζ_c)	Multiblade flapping (lag) coordinates: collective and first order cycling flapping (lag) components
θ	Equilibrium pitch angle= $\theta_o+\theta_s$ sint+$\theta_c$cost
ν_o,ν_s and ν_c	Uniform, side-to-side and fore-to-aft inflow perturbations
Ω	Rotor rotational speed in rpm
ω_ζ	Dimensionless ($1/\Omega$) uncoupled lag frequency
γ	Lock number
$(\cdot)$	d/dt

1. INTRODUCTION

Much research is still required in the measurement and prediction of stability margins of conceptual hingeless rotor models, particularly of inplane damping[1-3]. There are three main reasons for this situation. First, most research is not keyed to concomitant correlation between theory and experiment for verifying and improving the theory by isolating ingredients that participate in the correlation, and for resolving anomalous predicted and measured data[1]. Second, in most of the global programs and test configurations, though of design significance, the model complexity practically precludes the process of isolating such ingredients. Third, even when conceptual experimental models are used, the predicted data often refer to multipurpose global programs, in preference to developing an analysis package that is directly tailored to fit the conceptual model and that can be refined in stages to improve the correlation. In particular, such an evolving analysis is desirable for inplane damping for which the state-of-the-art of predicting merits considerable refinements[4-9]. When compared to global programs, such evolving analysis packages do not have the burden of unessential complexities and can fully exploit the intentionally built-in characteristics of the conceptual experimental model. Therefore, they provide better visibility for breaking the problem down into simpler components and thereby, for isolating those ingredients for a better and improved understanding of low-frequency instabilities.

Relatively few such evolving analyses with concomitant corroboration of test data have been conducted on low-frequency instabilities of isolated rotors.[1-3] Here, we study some basic aspects of such an analysis concerning the flap-lag stability of a three-bladed isolated rotor in hover and forward flight ($0\leq\mu\leq0.55$). The crucial lag regressing mode is emphasized, which is practically independent of the number of blades per se.[4]. The data base comprises nearly 1400 test points of damping and frequency values, and it includes a small portion of the forward flight data in stall ($\alpha>|12°|$). The theory is based on quasisteady aerodynamics with dynamic inflow in substall. Although it merits substantial refinements in stall, we have included some correlation in stall as well. Such an inclusion facilitates an improved interpretation of the correlation between measured and predicted data including anomalous data.

The correlation is oriented for a specific rotor model under untrim conditions and it is based on a linear theory. However, it is based on a comprehensive data base for different flight regimes of a model with intentionally built-in structural simplicity. Such a correlation should give generally applicable qualitative results on the adequacy of the linear theory when stall is not an issue and should promote further refinements. It may also promote additional insights in resolving for stall effects under the analytically demanding conditions of forward flight. The study is of particular significance to tail rotors with polar symmetry ($N \geq 3$) which operate untrimmed and which often encounter stall conditions as well.[7,8]

2. EXPERIMENTAL MODEL

The model tested was a three-bladed hingeless rotor with a diameter of 1.62 m. The rotor was designed to closely approach the simple theoretical concept of a hingeless rotor as a set of rigid, articulated blades with spring restraint and coincident flap and lead-lag hinges. This was accomplished by the "folded back" flexure design shown in an exploded view in Fig. 1. Taking the center of the flexural elements as the effective hinge point gives a non-dimensional hinge offset of 0.11 for the design. The blades were designed to be very stiff relative to the flexures so that the first flap and lead-lag modes involve only rigid body blade motion. The influence of the torsional degree of freedom was minimized by keeping the first torsion frequency as high as possible. In particular, the first torsion mode frequency was above 150 Hz non-rotating, insuring a rotating first torsion frequency of at least 9/rev over the entire rotor speed range tested. The rotor properties are summarized in Table 1.

The rotor had no cyclic pitch control, and collective pitch was set manually before each run. The blade pitch could be set by changing the angle of the blade relative to the flexure at the blade-flexure attachment, giving a structural coupling value of zero, or by changing the angle of the entire blade-flexure assmbly relative to the hub, giving a structural coupling value of one.

The test stand on which the rotor was mounted included a roll gimbal which could be locked out mechanically. Rotor excitation was accomplished through this gimbal by a 50 lb (11.2N) electromagnetic shaker. The stand was designed to be as stiff as possible so that the test would closely represent the case of an isolated rotor, however, the lowest frequency of the installed stand with the gimbal locked and the rotor mounted was found to be 31 Hz, somewhat lower than was desired. The entire test stand could be pitched forward with an electric actuator to control the rotor shaft angle. The shaft angle provided the only means of controlling the rotor loads at a given collective pitch and advance ratio. A photograph of the model installed in the wind tunnel is shown in Fig. 2.

3. ANALYTICAL MODEL

The analytical model consists of an offset-hinged rigid lag-flap model with flap and lag spring restraints at the offset hinge. The spring stiffnesses are selected such that the uncoupled rotating flap and lag natural frequencies

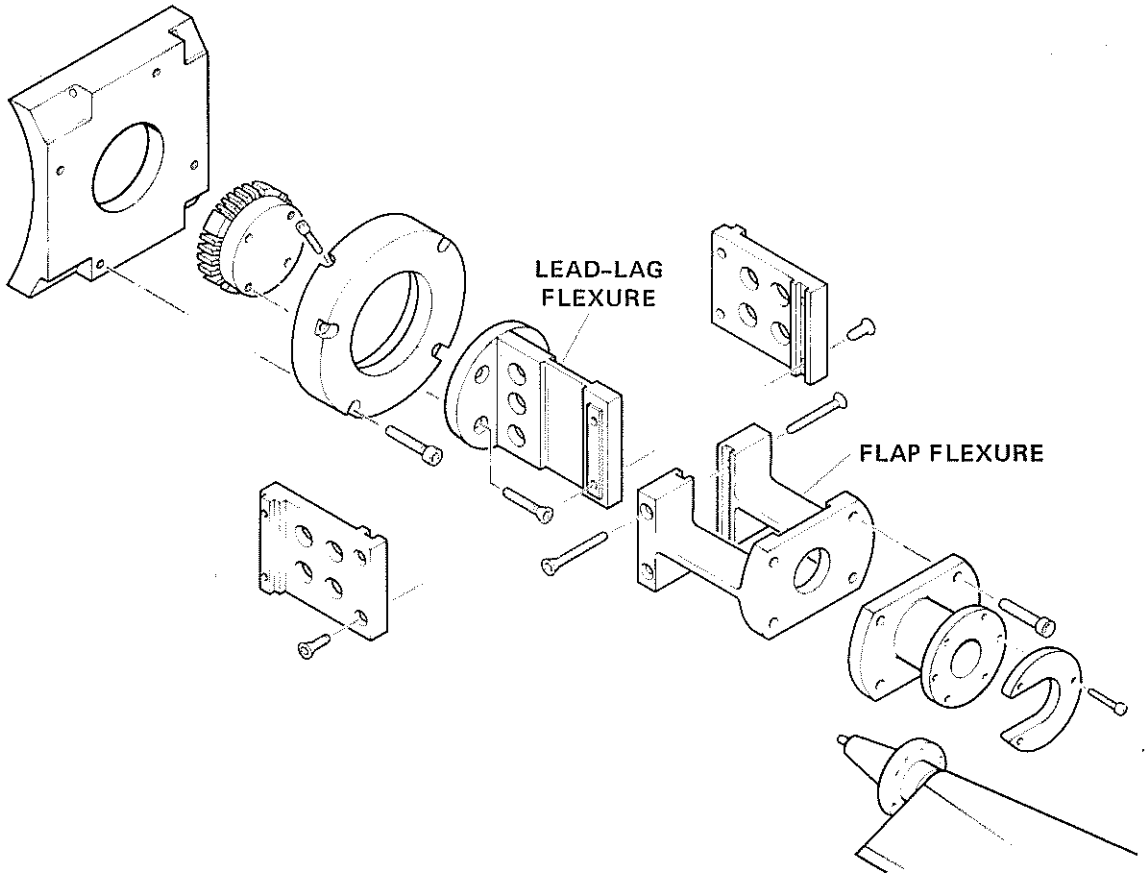

Figure 1. Exploded view of model flexure.

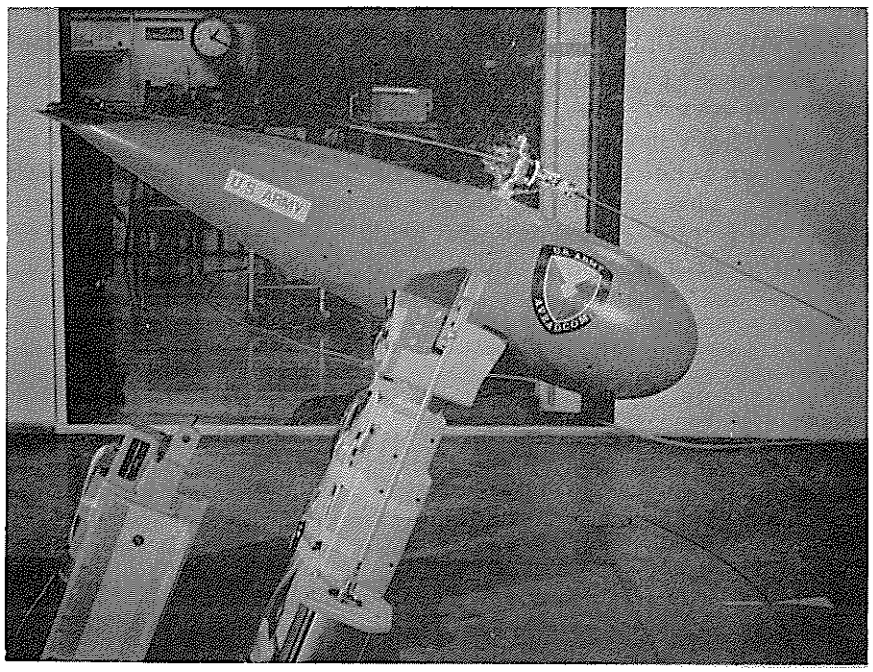

Figure 2. Model installed in the aeromechanics laboratory's 7-by-10-foot wind tunnel.

coincide with the corresponding first-mode rotating natural frequencies of the elastic blade. The effect of the hinge offset, which is 11.1% in lag and flap, is accounted for in rotor trim and stability analyses. The rotor is untrimmed, with an essentially unrestricted tilt of the tip path plane, as is typical of tail rotors. the rotor angular velocity is Ω, and with time unit $1/\Omega$, the azimuth angle of the first or the reference blade represents the dimensionless time t. The distribution of flexibility between the hub including flexures and the blade (outboard of the blade location where pitch change takes place) is simulated by an elastic coupling parameter R which is also referred to as the hub rigidity parameter. Basically, R relates the rotation of the principal axes of the blade-hub system and the blade pitch θ.

The blade airfoil aerodynamics is based on linear, quasisteady theory in substall (angle of attack $\alpha < |12°|$) without the inclusion of compressibility or other effects due to reversed and radial flow. Steady uniform inflow is assumed. The airfoil nonlinear section effects are neglected.[10-11] The dynamic inflow effects are included from a verified inflow model based on an unsteady actuator-disk theory---the Pitt Model.[5,9] The inflow model leads to a consistent rotor-wake description for rotors with three and more blades.[9] It has been recently verified on the basis of experimental correlation with low-thrust flap-response data, since pure flap-response provides a data base to pass a judgement on a particular inflow model.[5] The ordering scheme and computational details are as in references 4 and 12.

The equations of motion including the multiblade coordinate transformation are derived from symbolic manipulation[13,14]. For the three-bladed rotor, the 15x1 state vector comprises 12 multiblade components (β_0, $\dot{\beta}_0$, β_s, $\dot{\beta}_s$, β_c, $\dot{\beta}_c$, ζ_0, ζ_0, ζ_s, $\dot{\zeta}_s$, ζ_c, $\dot{\zeta}_c$) and 3 dynamic inflow components (ν_0, ν_s, ν_c). The completely automated mode identification is based on a Floquet eigenvector approach.[4,13,14] The stall region contours with $\alpha=|12°|$ are based on "untrim" values ($\theta_s=\theta_c=0$, cyclic flapping present).[10]

4. EXPERIMENTAL PROCEDURES

An experimental investigation of the rotor's lead-lag stability characteristics in hover and, especially, forward flight was conducted in the Aeroflightdynamics Directorate's 7-by-10 foot (2.1-by-3.0 m) wind tunnel at the NASA-Ames Research Center. The data was collected in two tunnel entries, the first in the summer of 1982 and the second in the summer of 1983. The model's configuration and the test procedures used were the same for both tests. The only exception to this is that for the 1982 test the hover data was taken with the wind tunnel test section doors open and the windows removed in an attempt to reduce recirculation effects. In 1983 the hover data were taken incidental to forward flight data so the windows were left in place and doors were closed. The rotor plane itself was located about 0.63 rotor diameters above the test section floor (with the shaft vertical), and so the influence of recirculation and ground effect on the hover data, especially at the higher values of blade pitch and rotor speed could be significant.

For each data point obtained the blade pitch was set manually and the rotor was tracked. The rotor was then brought up to speed and wind tunnel dynamic pressure increased to obtain the desired advance ratio while adjusting the shaft angle to keep the rotor flapping loads within limits. Once at the test condition, the roll gimbal was unlocked and the shaker was used to excite the

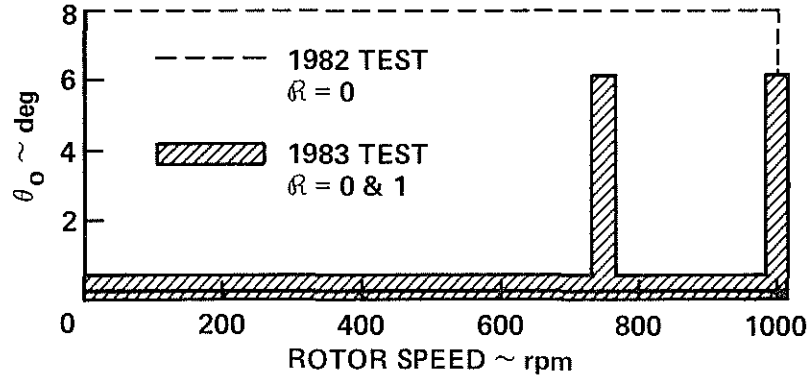

3(a) Hover tests.

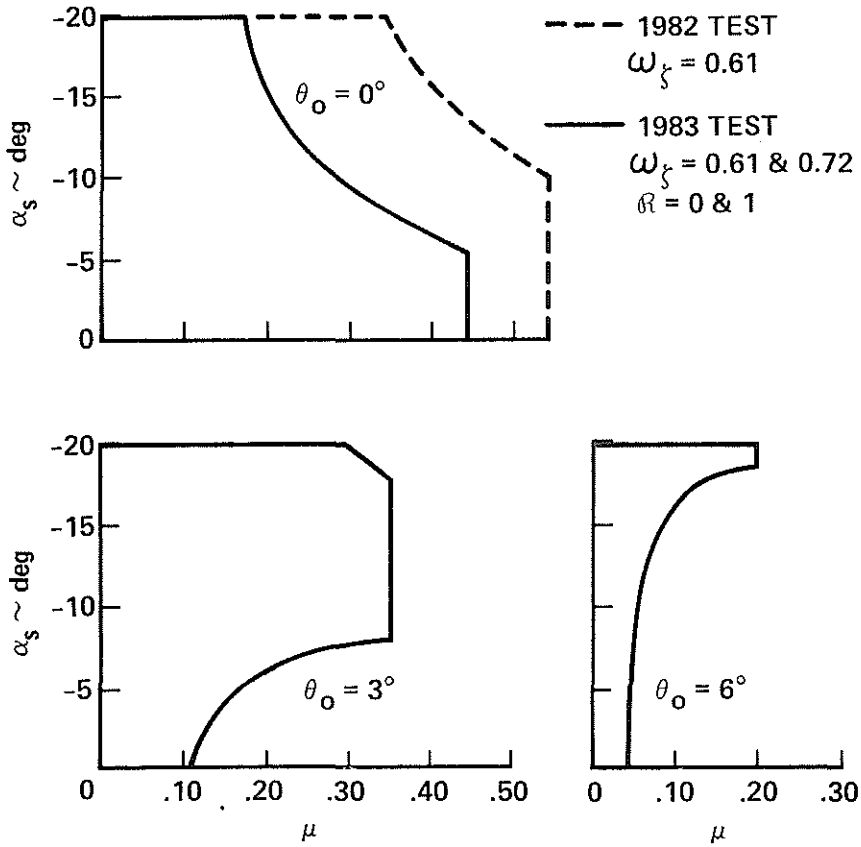

3(b) Forward flight tests.

Figure 3. Conditions tested.

model at the appropriate frequency. When a good level of excitation was evident in the output of the lead-lag bending gages the shaker was cutoff, the roll gimbal locked out, and then transient data acquistion commenced. The data itself was digitized on-line with a sample rate of 100 Hz and a total record length of 5.12 seconds. The data was then transformed to the fixed system coordinates. Spectral analysis and the moving block technique[15] were used to determine the frequency and damping of the response. At least two data points were obtained at each test condition and the scatter between the measurements was found to be very small.

Progressing and regressing lead-lag mode data were obtained for the hover test conditions, but above about 600rpm the progressing mode was found to be contaminated by coupling with the lower stand mode. Because all of the forward flight conditions tested were above this rotor speed, no progressing mode data were obtained. The regressing mode data should be representative of isolated blade results over the entire rotor speed range tested and appears to be of very good quality. The hover test envelopes for both the 1982 and 1983 tests are shown in Fig. 3(a) and the forward flight test envelopes are shown in Fig. 3(b). The edges of the forward flight envelopes were set by the maximum allowable rotor flapping loads.

Table 1: Model Properties

Number of Blades	3
Radius	0.81 m
Chord	0.0419 m
Airfoil Section	NACA 23012
Lift Curve Slope	5.73
Profile Drag Coef.	0.0079
Non-dimensional Hinge Offset	0.111
Blade Inertia About Hinge	0.01695 kg-m^2
Blade Mass Center Distance from Hinge	0.188m
Blade Mass (Outboard of Hinge)	0.204 kg
Non-rotating Flap Frequency	3.09 Hz
Non-rotating Lead-lag Frequency	7.02 Hz
Lead-lag Structural Damping Ratio	0.2% crtical
Lock Number γ	7.54

5. CORRELATION OF THEORY AND DATA

We, now come to presenting the correlation between the measured and predicted data in hover and forward flight ($0 \leq \mu \leq .55$). If not stated otherwise, the predicted data based on a linear theory in substall includes dynamic inflow. Further, the percent stall area of the rotor disk is used as a means of quantifying the stall effects on the correlation between theory and data. Figures 4 to 6 refer to the hovering conditions with Ω =1000 rpm and R=0 for four values of collectives: θ_o= 0°, 4°, 6° and 8°. By comparison, the data in forward flight is broader in scope, as presented in figures 7 to 20 for θ_o =0°, 3° and 6°. Here, for each pitch setting, we have basically four test cases---two rotational speeds (Ω= 1000 and 750 rpms) in combination with two flap-lag coupling parameters (R=0 and 1.)

In figure 4, we show the frequency correlation for the lag regressing and progressing modes. The excellent correlation between theory and data is

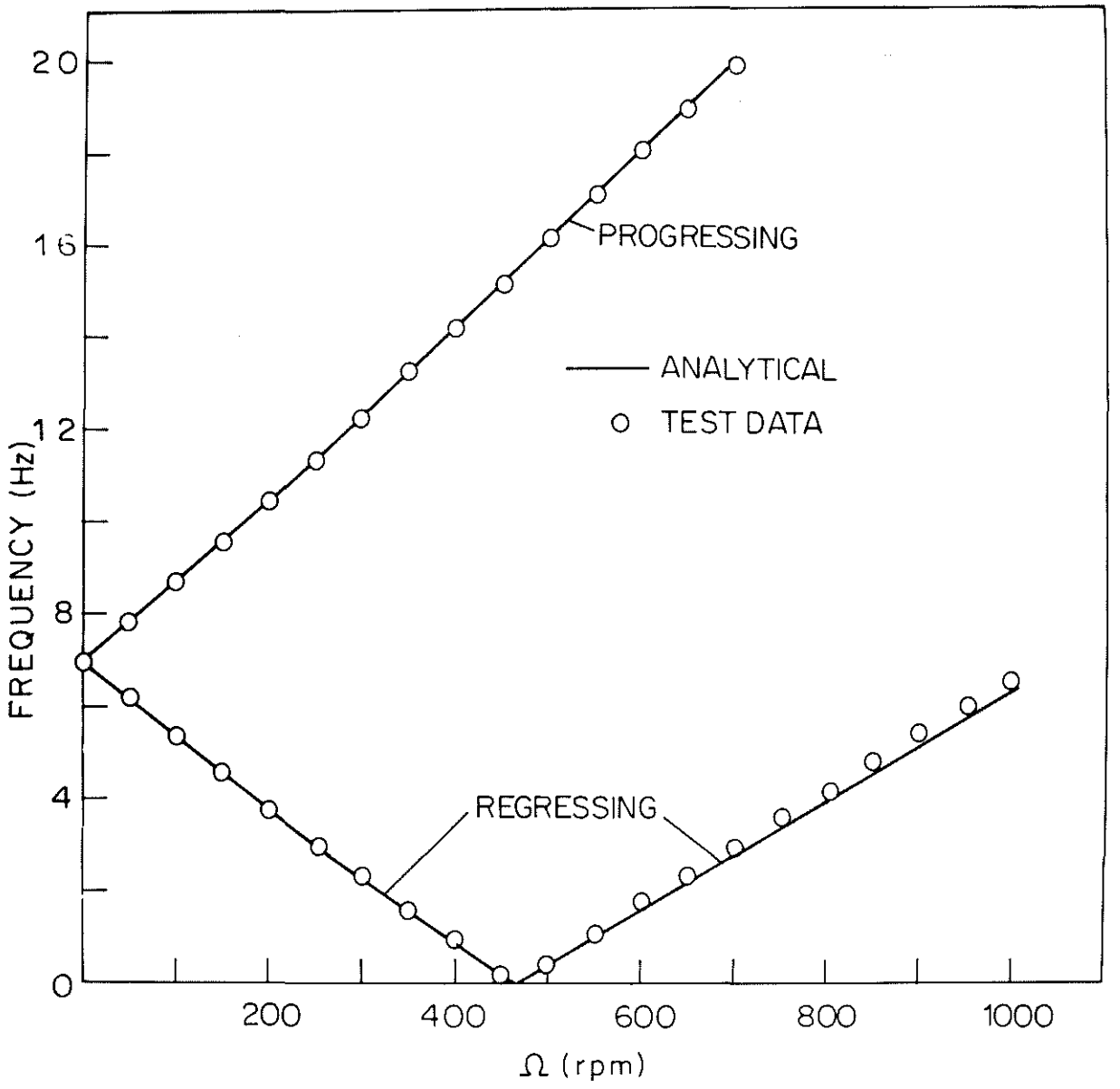

FIG. 4 CORRELATION OF MEASURED FREQUENCY DATA WITH PREDICTED VALUES ($\theta_0 = 0°$, $\mu = 0$)

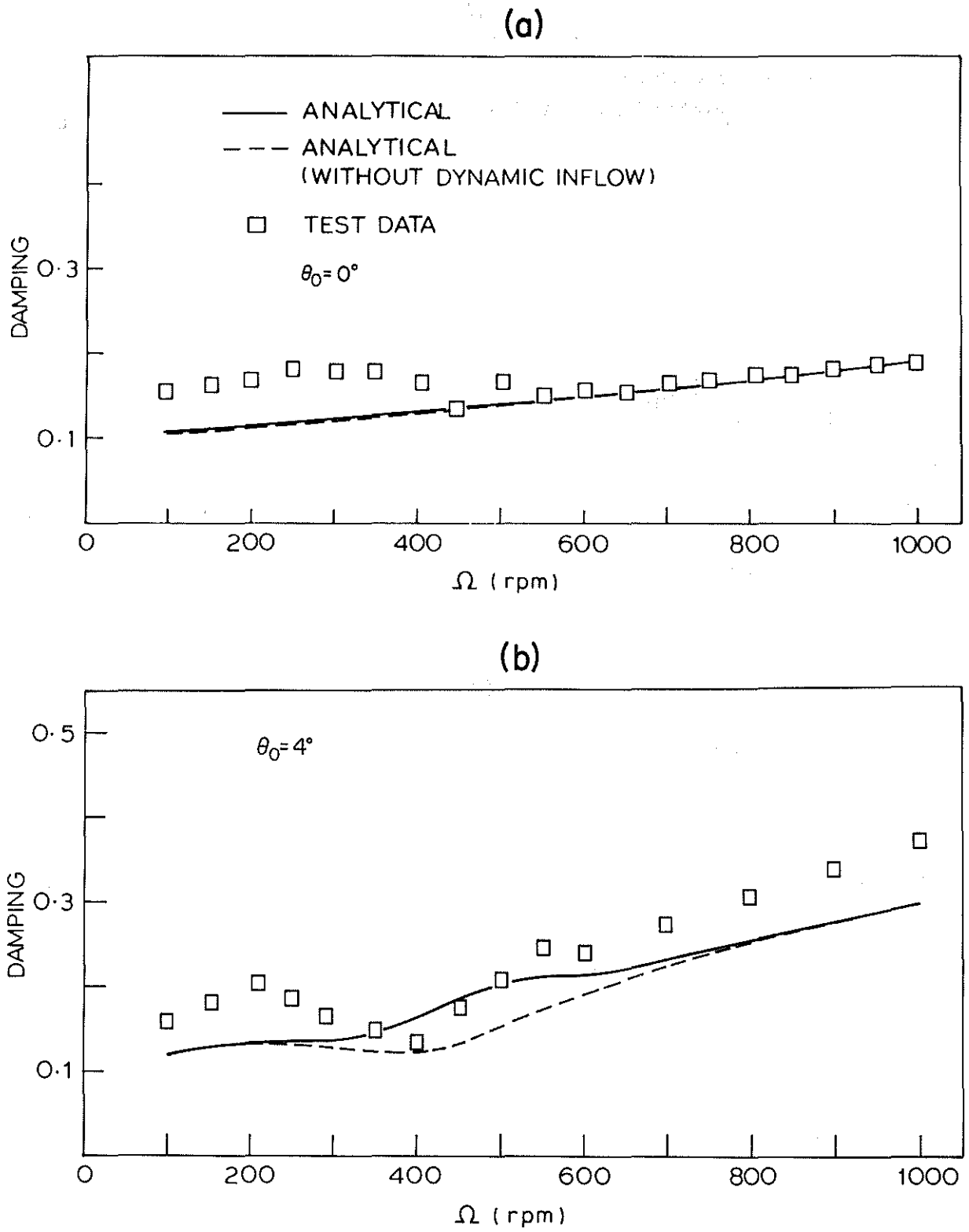

Fig.5 CORRELATION OF MEASURED LAG REGRESSING MODE DAMPING WITH PREDICTED VALUES IN HOVER

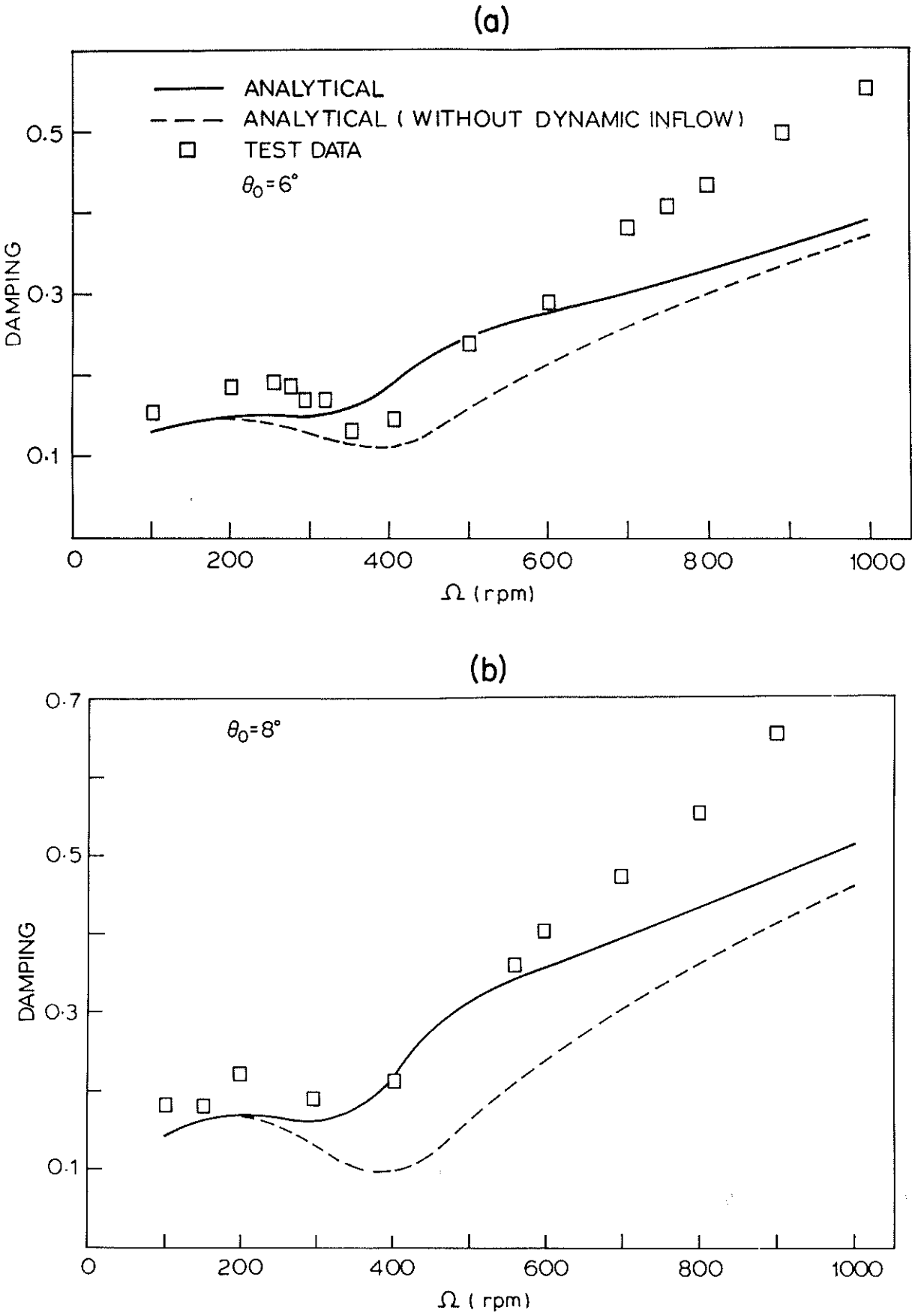

Fig.6 CORRELATION OF MEASURED LAG REGRESSING MODE DAMPING WITH PREDICTED VALUES IN HOVER

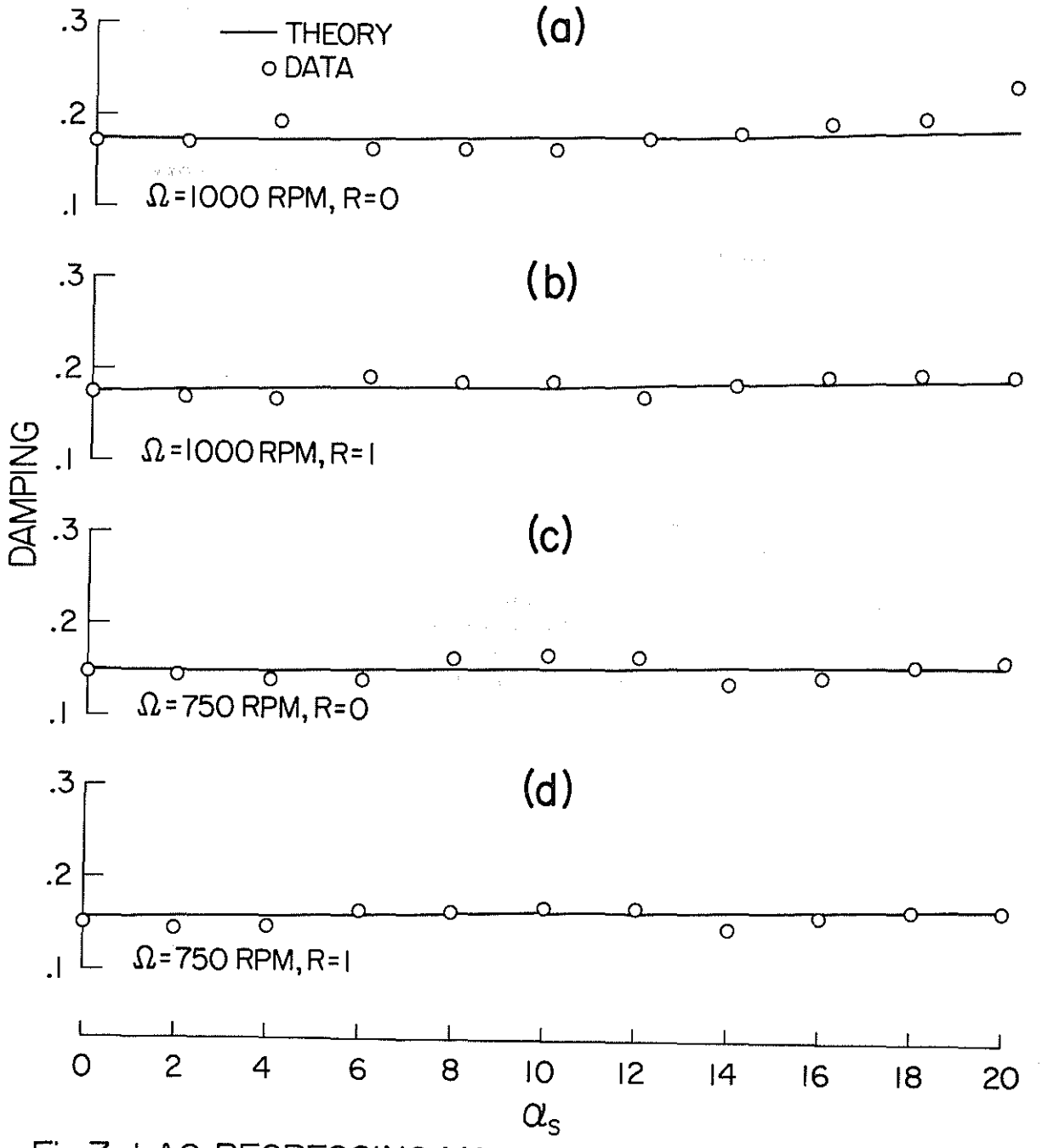

Fig.7 LAG REGRESSING MODE DAMPING, $\mu = 0.1$ and $\theta_0 = 0°$

noteworthy for both the modes. It is good to mention that the improvement in correlation due to including dynamic inflow is at best marginal for the frequency correlation. Continuing, in figures 5 and 6, we show the lag regressing mode damping versus the rotor rotational speed Ω. While the dotted lines refer to the theory without dynamic inflow, the full lines refer to the theory with dynamic inflow. It is significant that for zero pitch setting in figure 5a, excellent correlation is obtained without and with dynamic inflow, except for minor discrepancies between theory and data for very low rotational speeds (say, Ω<300rpm). For θ_o=4°, 6°and 8°, as presented in figures 5b and 6, the inclusion of dynamic inflow improves correlation. However, for Ω > 800 rpm, the theory deviates from the data and that deviation increases with increasing blade pitch (compare figure 5b with figure 6a). The 1.62-m model was tested in a 2.13 x 3.05 meter test section. With increasing rotor speed and blade pitch, increasing recirculation and data scatter were observed. Further, since the model height to rotor diameter was 0.63, it is reasonable to expect minor ground effect on induced flow as well. In particular, the recirculation effects affect the data and, perhaps account for the increasing differences between theory and data in figures 5b and 6. Overall, the data are in general agreement with theory.

It is convenient to present the forward flight data in four stages. In the first three stages we present damping correlations respectively for θ_o=0°(figures 7 to 11), for θ_o= 3° (figures 12 to 15) and for θ_o= 6° (figures 16 to 18). In the fourth stage, we study frequency correlation for θ_o= 0°, 3° and 6° (figure 19) and the need to resolve anomalous predicted data (figure 20).

Figures 7 and 8 show the lag regressing mode damping for μ=0.1 and 0.2 respectively. The superb correlation between theory and data attests the adequacy of the linear theory well within substall (per cent stall area is much less than 10). To elaborate, we present stall regions in figure 9 for $0.2\leqslant\mu\leqslant0.5$. And once again, we consider figure 8, say, for Ω= 1000 rpm and R=0. For this case, the data are available for $0\leqslant\alpha_s\leqslant16°$, see figure 8a. It is instructive to observe that the stall region which is about 6% for α = 16°, increases to about 9% for α =20°; see figure 9a. This increase reflects the fact that for θ_o= 0°, the angle of attack increases with increasing shaft angle α_s, roughly as a function of $\mu\alpha_s$. However, the data in figures 7 and 8 are well within sub stall, due to μ being relatively small.

Before we take up high advance ratio cases (μ>0.25) it is helpful to revert to the stall regions in figure 9. It is seen that for μ= 0.3 and α_s= 12° and for μ =0.4 and α_s= 8°, more than 10% of the rotor disk is in stall. Moreover, the validity of the linear theory for μ=0.5, as seen from figure 9d, is suspect even for α_s>4°. With this as background, we take up figure 10 (μ= 0.3, $\alpha_s\leqslant10°$) and figure 11 (μ= 0.4, $\alpha_s\leqslant6°$). To isolate the role of stall in the correlation, we consider as typical samples, figures (10a) and (11a) which refer to Ω = 1000 rpm and R=0. While the maximum value of shaft tilt or $\alpha_{s,max}$= 8° in figure 10a, $\alpha_{s,max}$=4°in figure 11a. For these two cases the percent stall region is about 6, as seen from figure 9. In general, stall is not an issue for the eight cases presented in figures 10 and 11, as was the case in figures 7 and 8. Thus, in summary, the data in figures 7, 8, 10 and 11 exhibit superb correlation and demonstrate the adequacy of the linear theory well within substall.

Thus far, we presented the correlations in hover (figures 4 to 6) and in forward flight (figures 7,8, 10 and 11). It is instructive to compare these two sets of correlations. Overall, it is seen that the correlations in forward flight are relatively better. For example, compare figure 7 with figure 5a,

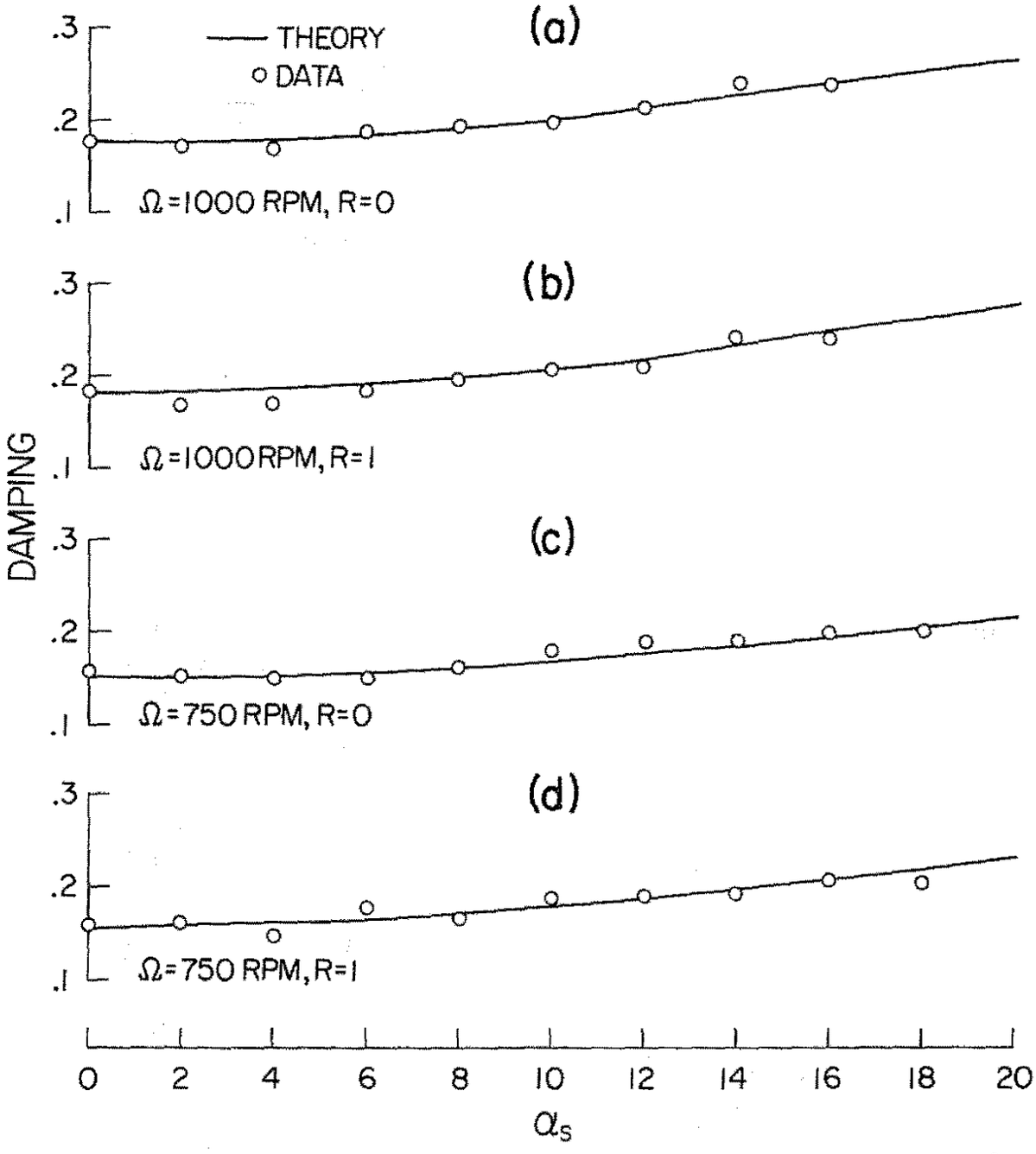

Fig.8 LAG REGRESSING MODE DAMPING, $\mu = 0.2$ and $\theta_0 = 0°$

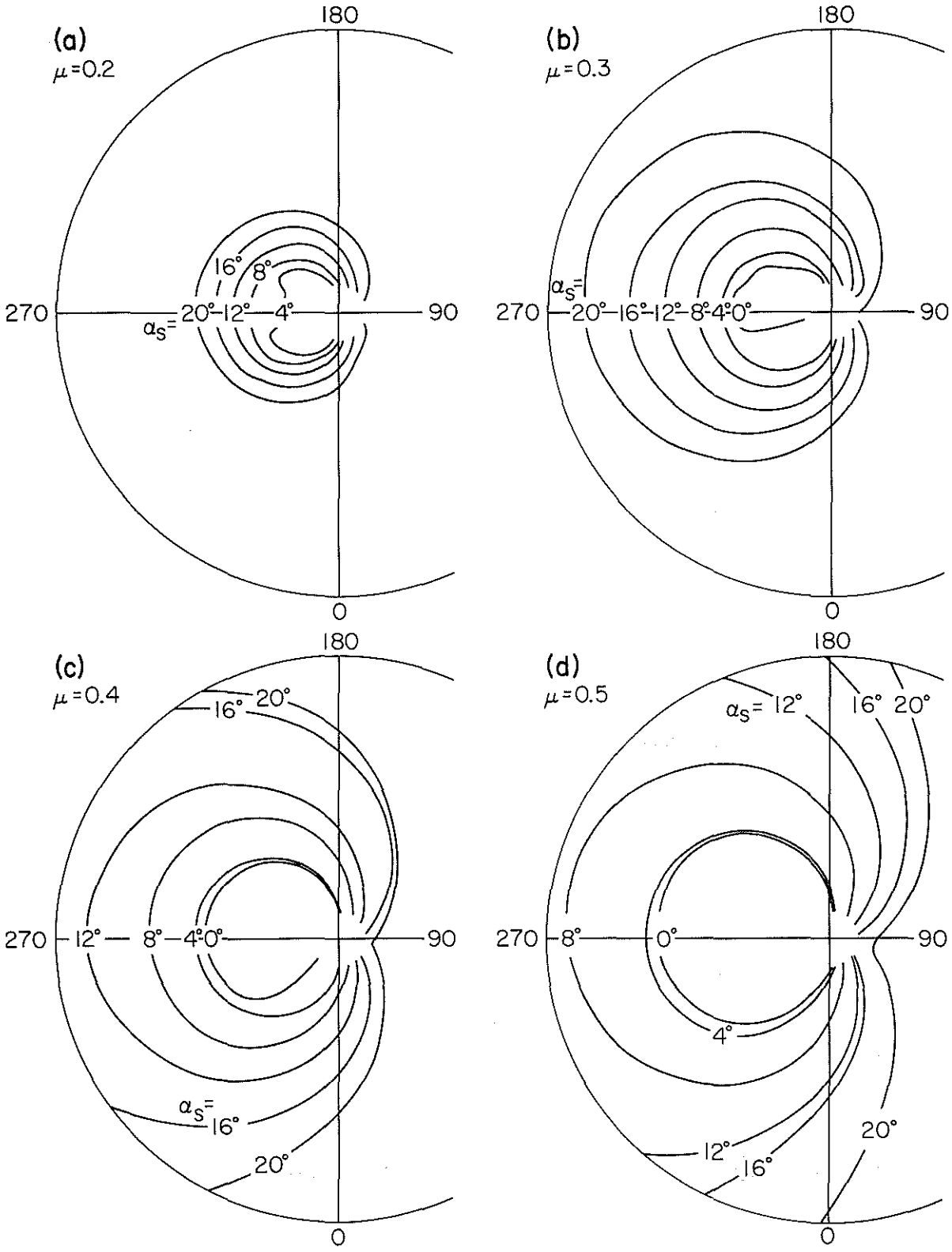

Fig.9 STALL REGIONS, $\theta_0 = 0°$ and $\Omega = 1000$ RPM

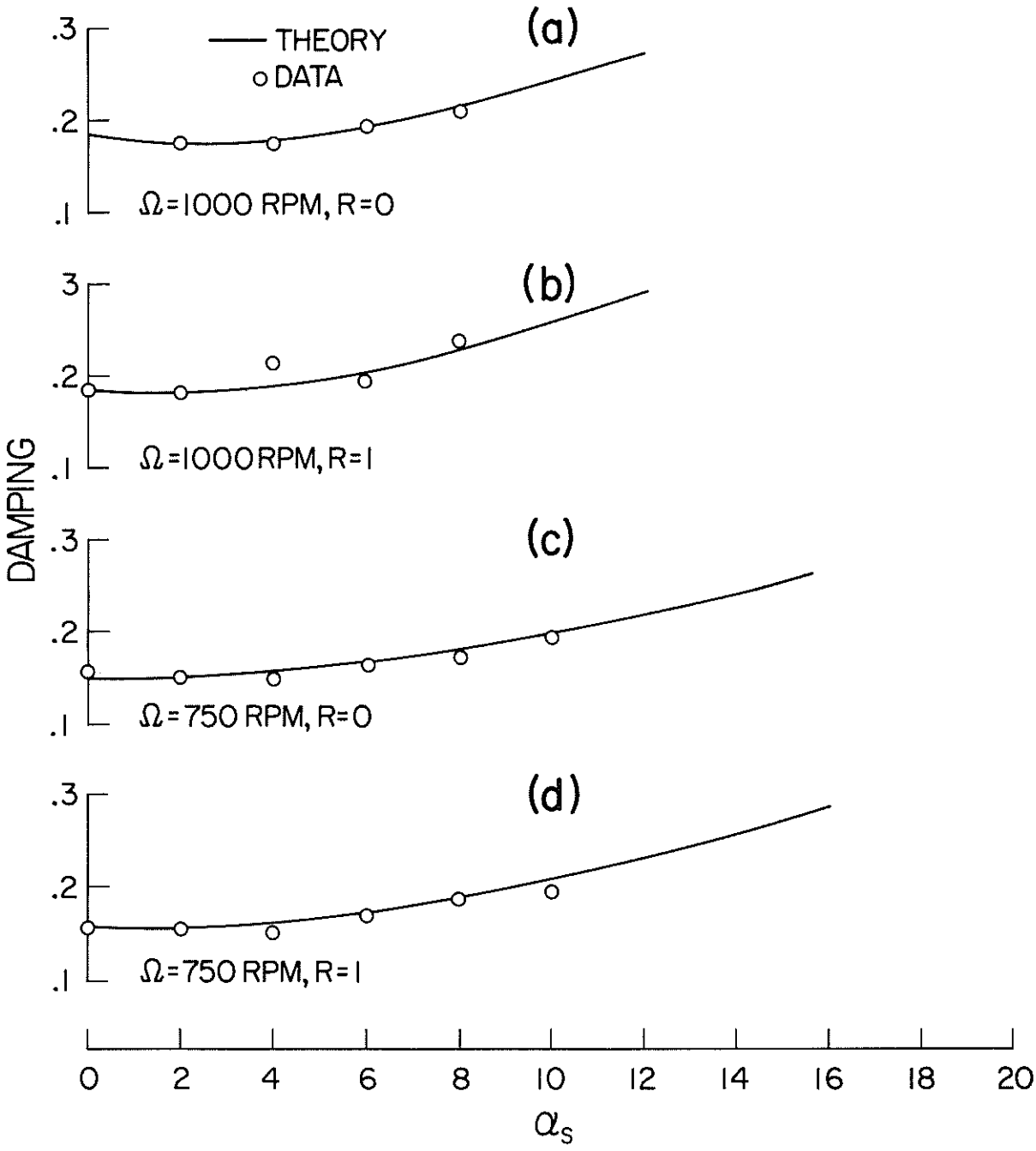

Fig.10 LAG REGRESSING MODE DAMPING, $\mu = 0.3$ and $\theta_0 = 0°$

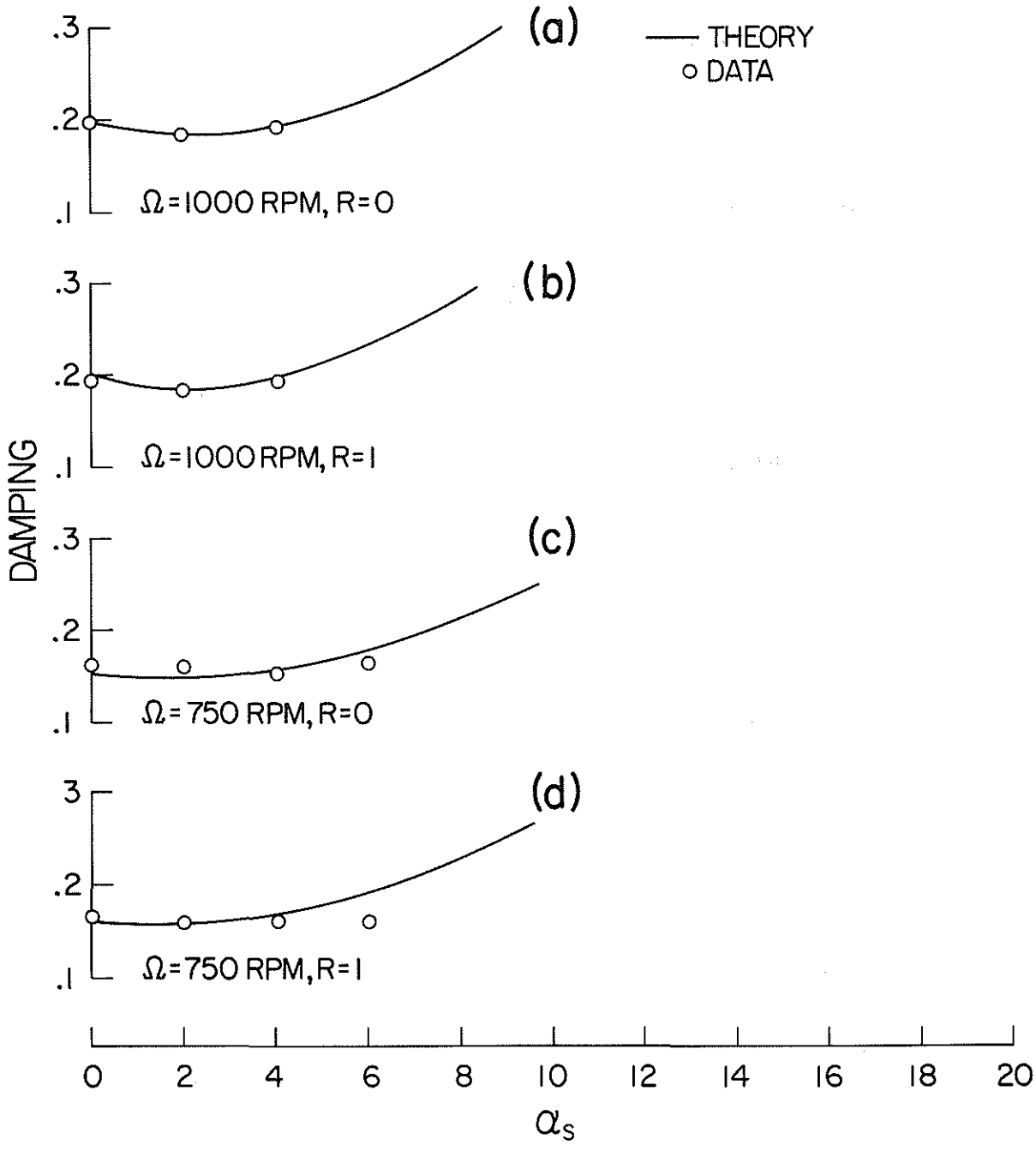

Fig.11 LAG REGRESSING MODE DAMPING, $\mu = 0.4$ and $\theta_0 = 0°$

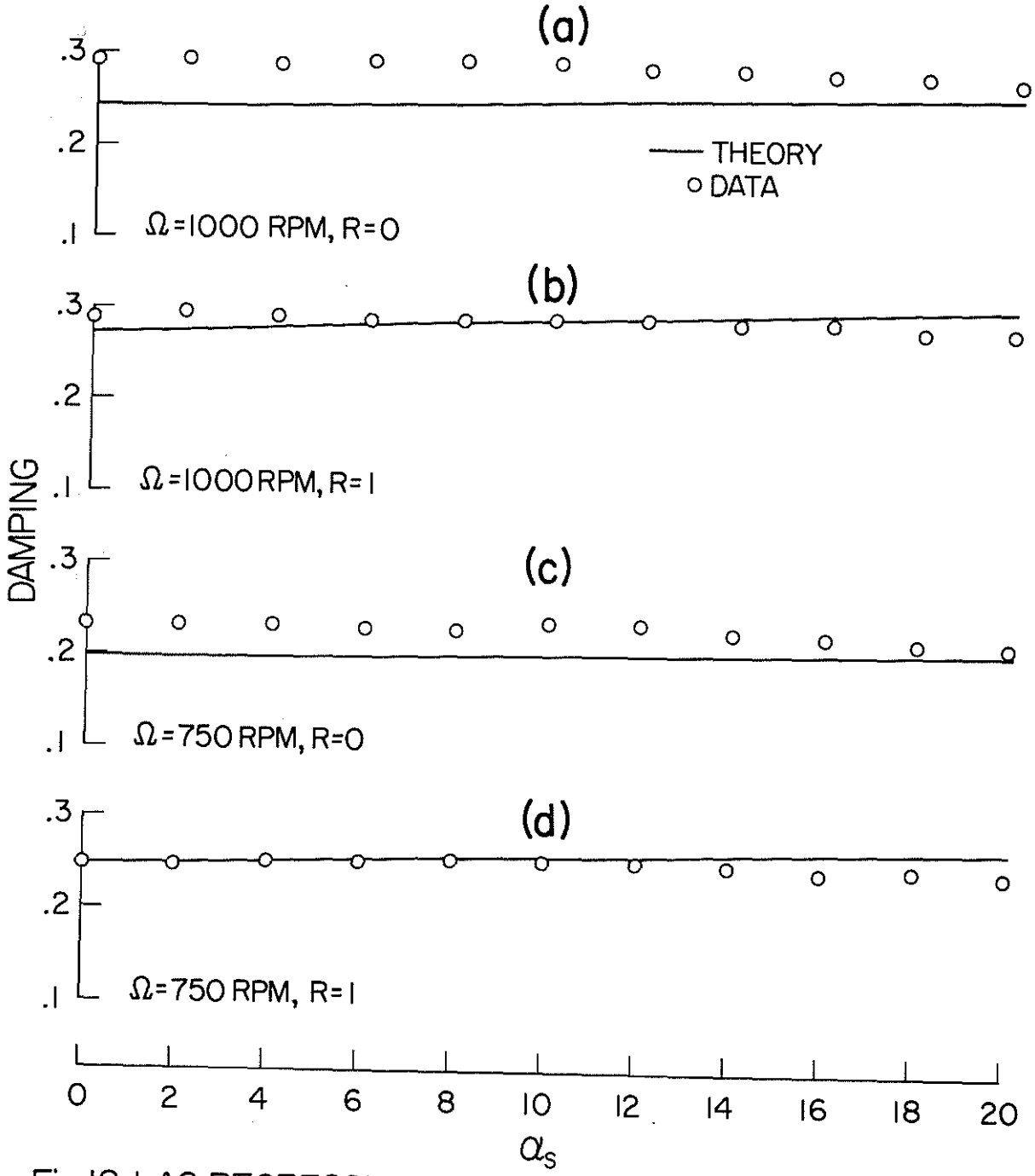

Fig.12 LAG REGRESSING MODE DAMPING, $\mu = 0.1$ and $\theta_0 = 3°$

both figures referring to zero pitch condition. This is due to the fact that the forward flight data are found to be of better quality. As noted in conjunction with the hover-data correlation, this fact reflects the relatively smoother rotor flow in forward flight than that in hover. This is further demonstrated by the repeatability of data in forward flight with relatively much less scatter.

As mentioned earlier, figures 12 to 15 refer to θ_o=3°, the second stage of data presentation in forward flight. While figures 12, 13 and 15 respectively refer to μ= 0.1, 0.2 and 0.3, figure 14 refers to stall region plots, as in figure 9. For the data in figure 12, stall ceases to be an issue, since the maximum stall region hardly exceeds 2% and the overall correlation for all the four cases is very good. It is worth noting that the correlation for the case with R=1 is relatively better when compared to the case with R=0. Although this trend is not consistantly maintained for the remaining sets of data (e.g. figure 13) we offer the following comment in passing. Usually, the rigid flap-lag blade model with R=0 (a soft hub with a rigid blade, with all the flexibility in the hub) is slightly a better model than the corresponding model with R=1 (a rigid hub with all the flexibility in the blade). After all, the simulation of root flexural flexibility by concentrated springs is more valid than the simulation of blade flexibility by concentrated springs. Yet, the data in figure 12 seems to indicate that the rigid blade-model with R=1 is equally viable.

For the data in figure 13 (μ=0.2, θ_o= 3°), stall is a minor issue. For example, for Ω=1000 rpm and R=0, the maximum per cent stall region is about 6. The correlation is very good for about α_s<16°. However, for α_s>18°, the theory deviates from the data. We suspect that non-uniform steady inflow and, to a much lesser extent, stall are contributing to the deviation. Before we take up the high advance ratio cases, it is good to study the role of stall, as typified in figure 14. It is seen that for μ=0.3, stall is a major factor for relatively high shaft angles. For example, for μ= 0.3 and α_s= 14°, nearly 10 % of the rotor disk is in stall and the stall region rapidly increases with increasing α_s, particularly for α_s>14°. Although data are not available for μ> 0.35 (see the data envelope in figure 3), figure 14c and 14d respectively, show that for μ=0.4 the linear theory is inadequate for α_s>10° and that for μ= 0.5, the linear theory is suspect, except over a narrow range of shaft angles close to 4°.

We, now, take up figure 15 which refers μ=0.3. Here also, well within substall (per cent stall region<<10), the theory correlates reasonably well with the data. As expected, the correlation degrades with increasing α_s, particularly for α_s>14°. This should not surprise us since for α_s=20°, the per cent stall region is close to 14. Stall is a prime candidate for this degradation.

We, now, take up the correlation for θ_o=6°, the third stage of data presentation, as typified in figures 16 to 18. While figures 16 and 17 respectively refer to μ= 0.1 and 0.2, figure 18 shows the stall regions. Except for Ω= 750 rpm and R=0 in figure 17b, the correlation in figures 16 and 17 is at best qulitatively accurate. Stall is not an issue here, since for μ=0.1 and 0.2, the stall region hardly exceeds 5% of the rotor disk. Isolating the issues for the deviation between theory and data merits further investigation. However, at low advance ratios (μ<.2) the model with increasing pitch setting and shaft tilt are expected to encounter highly nonuniform steady inflow, although the theory is based on uniform steady inflow. The correlation for μ=0.05 is not shown here. However, it was found that the deviation between theory and data for very small

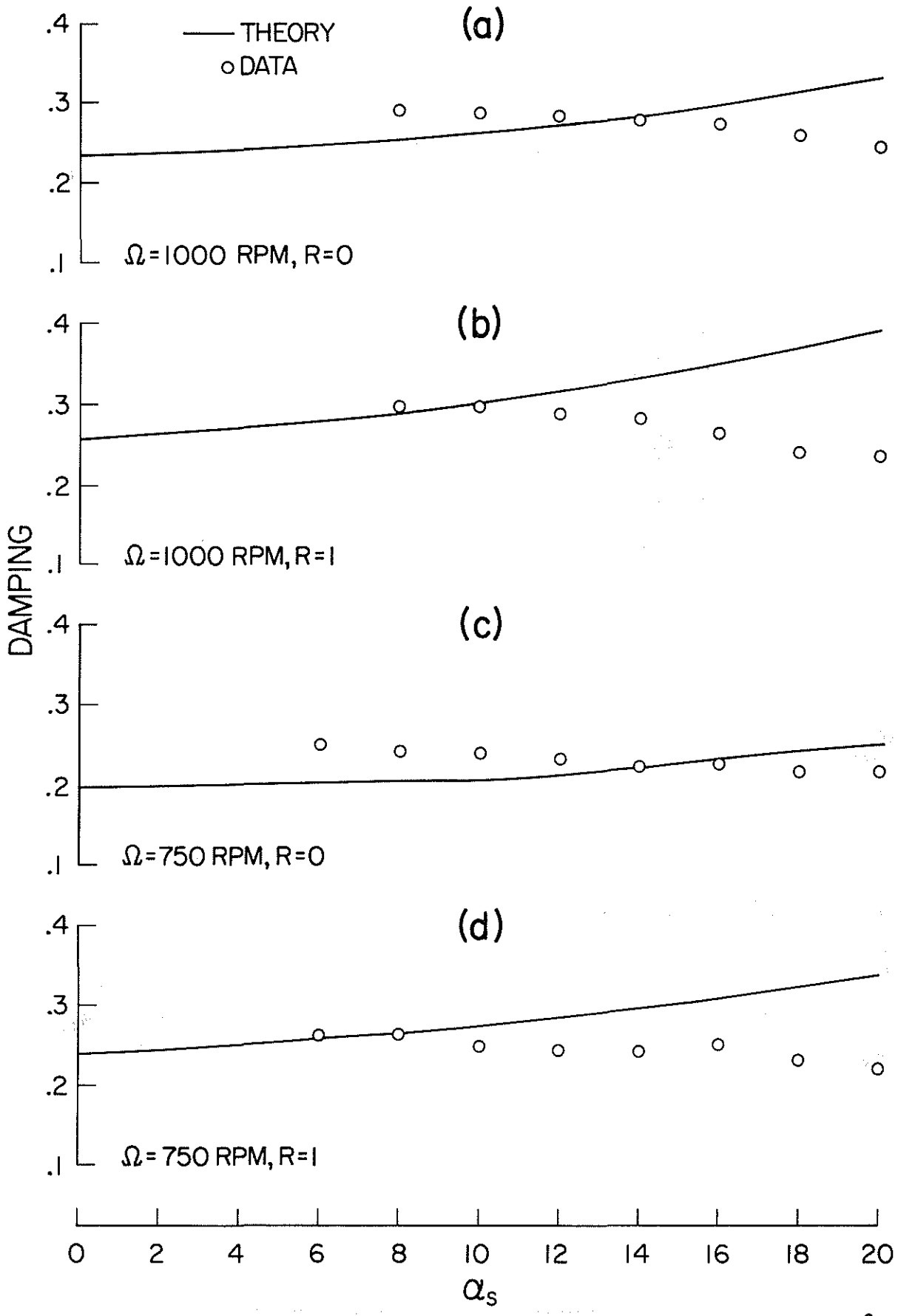

Fig. 13 LAG REGRESSING MODE DAMPING, $\mu=0.2$ and $\theta_0=3^\circ$

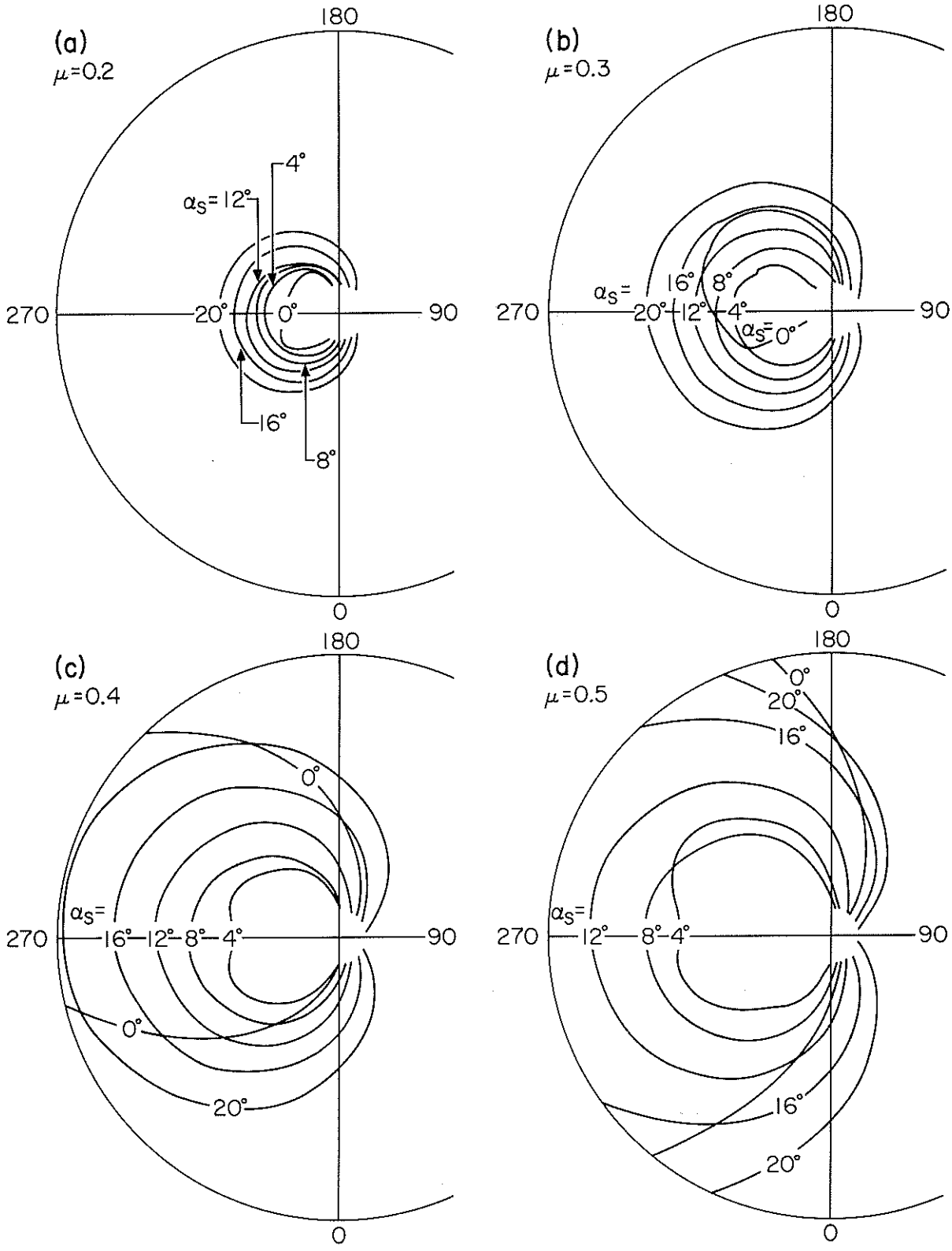

Fig.14 STALL REGIONS, $\theta_0 = 3°$ and $\Omega = 1000$ RPM

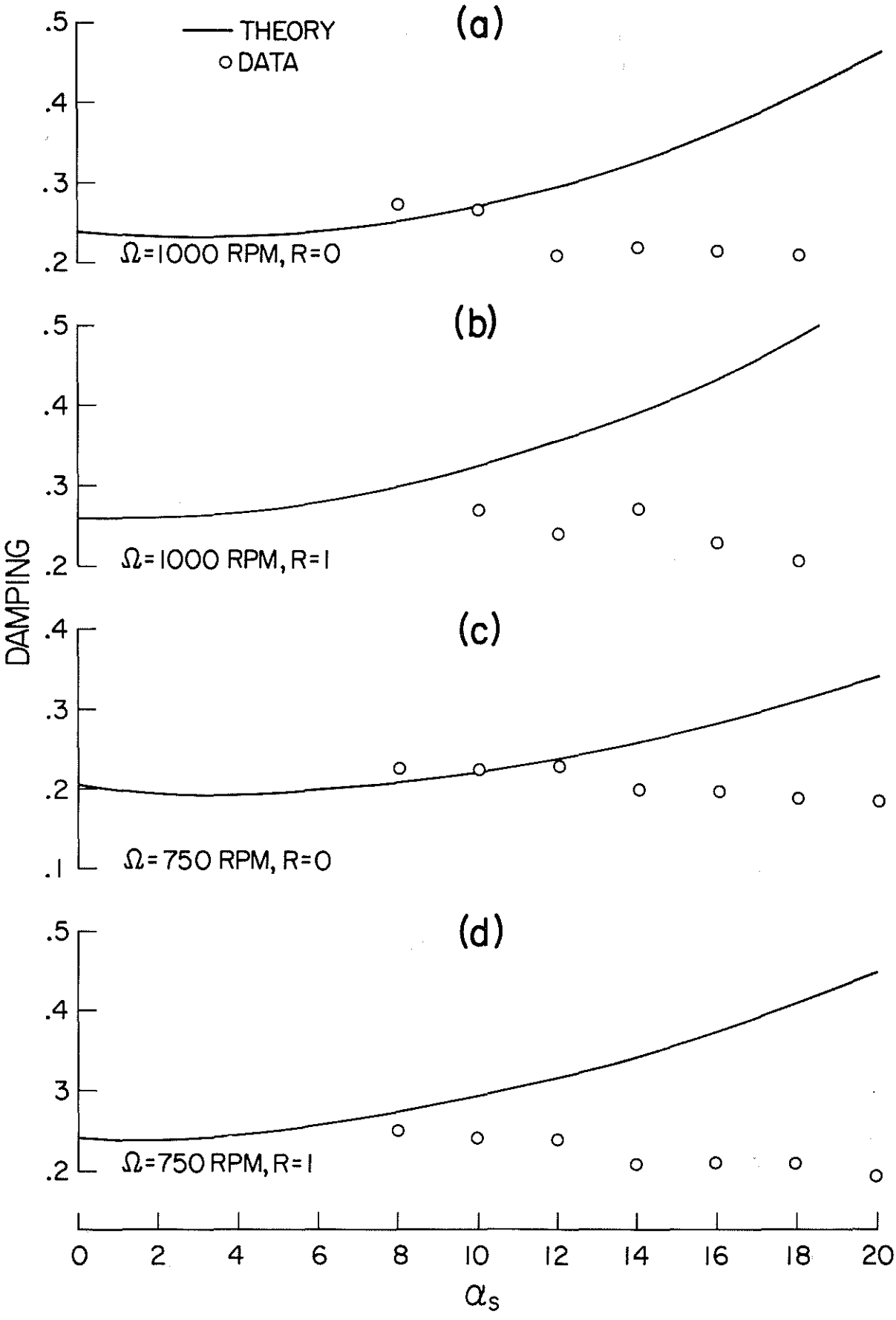

Fig.15 LAG REGRESSING MODE DAMPING, $\mu = 0.3$ and $\theta_0 = 3°$

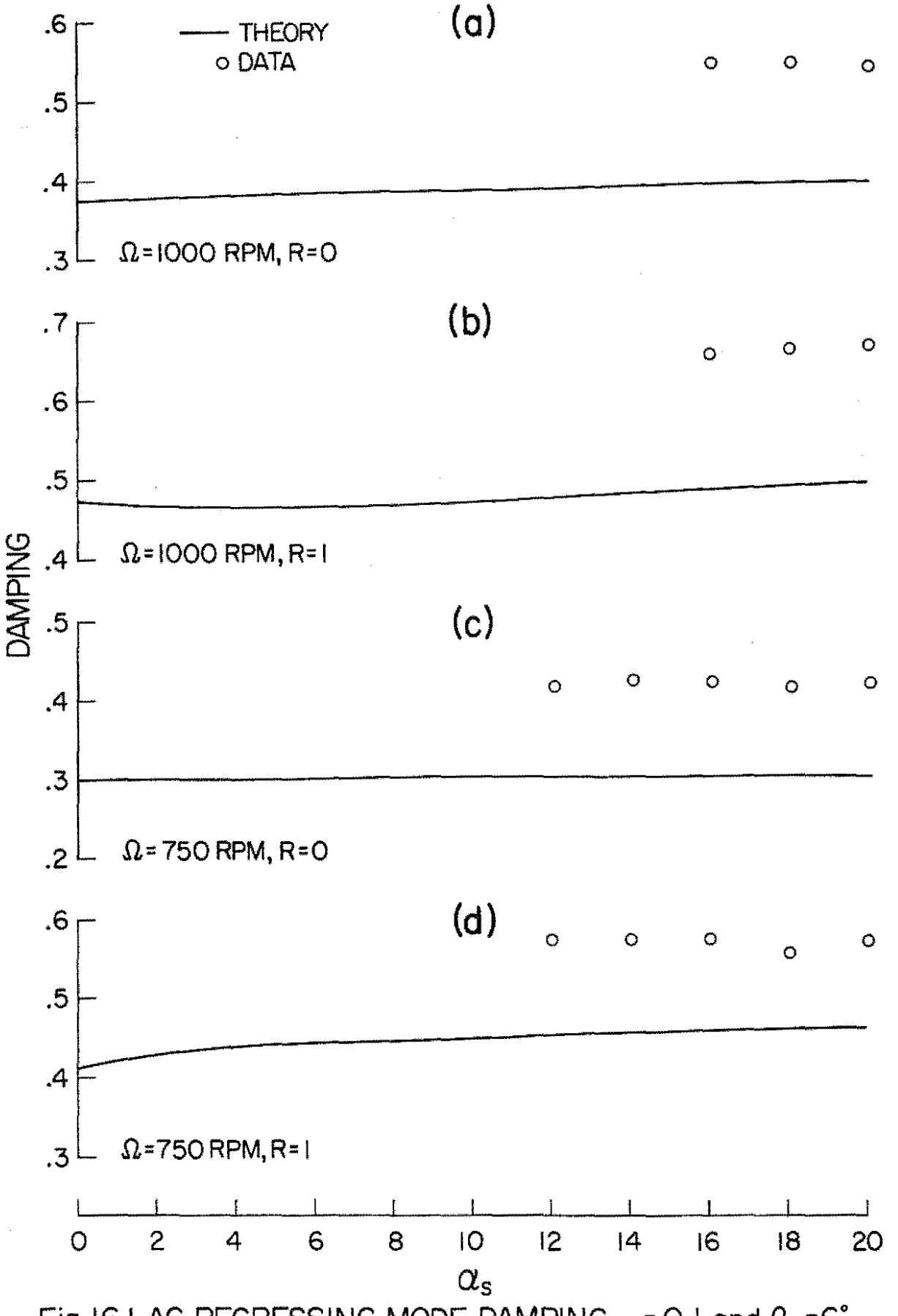

Fig. 16 LAG REGRESSING MODE DAMPING, $\mu = 0.1$ and $\theta_0 = 6°$

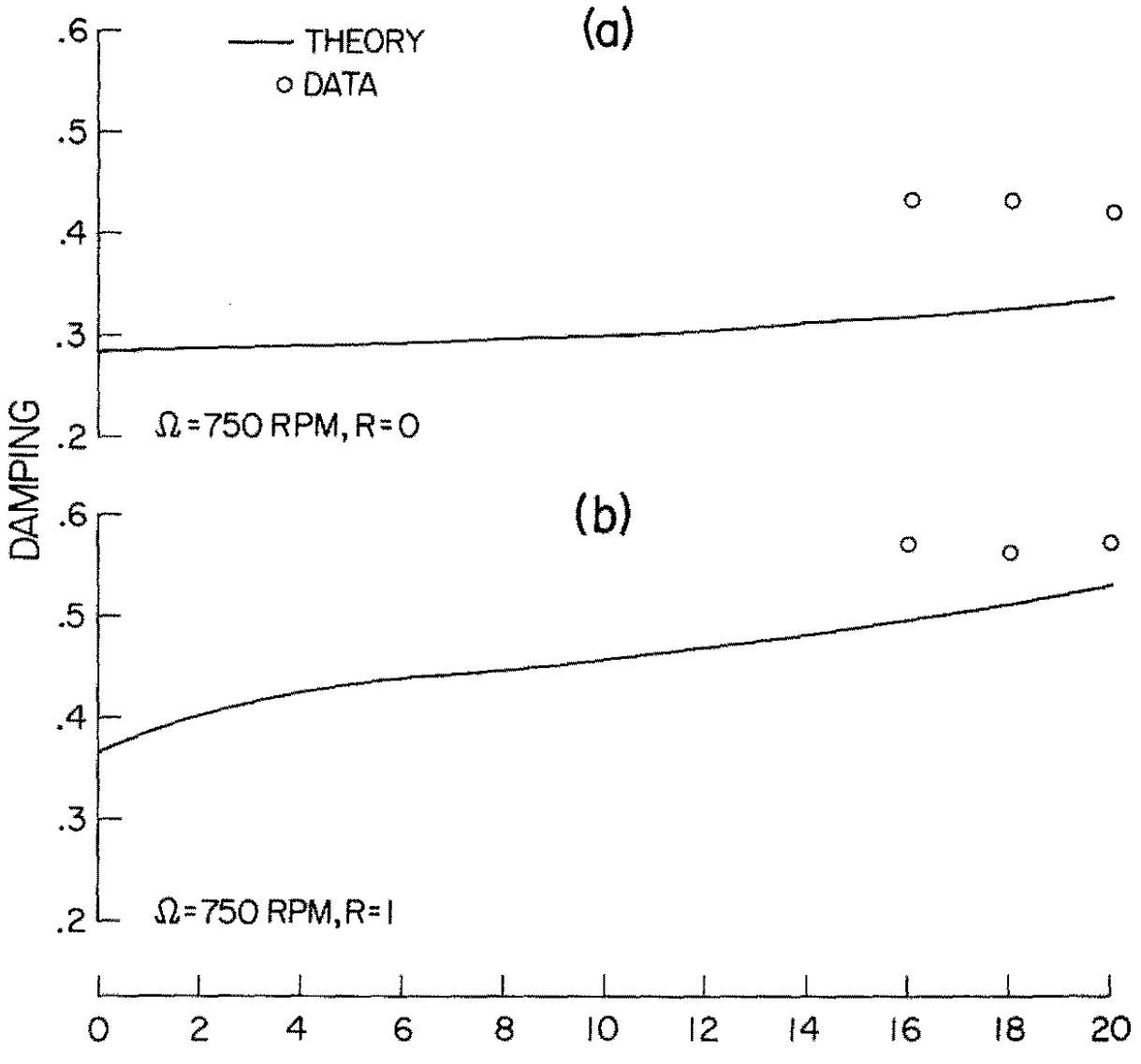

Fig.17 LAG REGRESSING MODE DAMPING, $\mu = 0.2$ and $\theta_0 = 6^\circ$

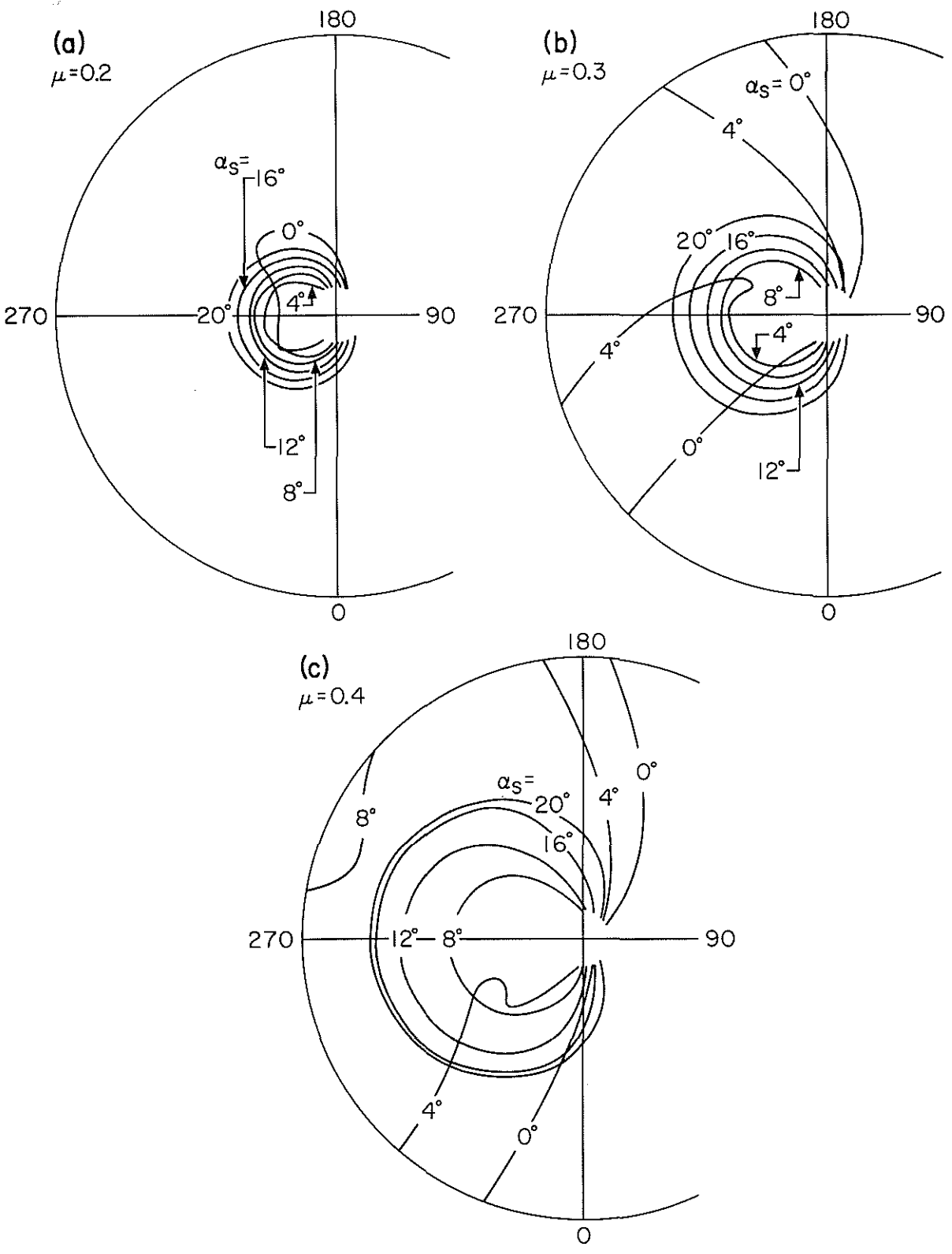

Fig.18 STALL REGIONS, $\theta_0 = 6°$ and $\Omega = 1000$ RPM

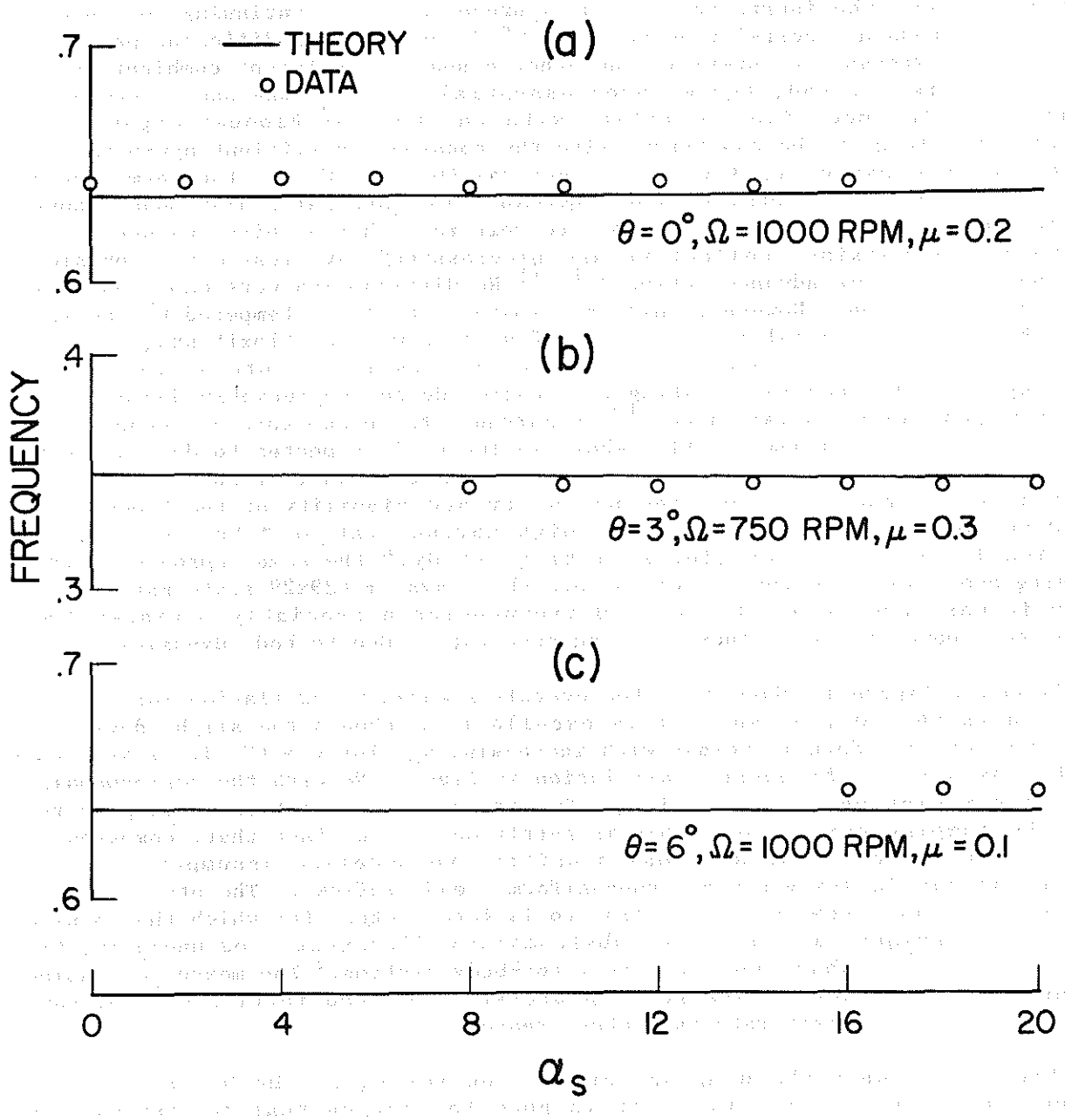

Fig. 19 LAG REGRESSING MODE FREQUENCY CORRELATIONS, R=0.

advance ratios ($0.0 \lesssim \mu \lesssim 0.1$) decreases with increasing μ ($\mu > 0.2$). (For example compare figure 16b with figure 17b.) Such a deviation shows that the present theory refined to include the effects of non-uniform steady inflow, should provide a means of uniquely isolating those effects. Coming to figure 18, we see that stall, though of minor consequence for $\mu = 0.2$, becomes a dominant factor for $\mu=0.4$. Even for $\mu = 0.3$, the linear theory is applicable over a restricted range of shaft angles, say $\alpha_s > 4^\circ$. (For $\theta_o=6^\circ$, data are available for $0.05 < \mu < 0.2$, as seen from figure 3).

Finally, we take up frequency correlation and the need to resolve anomalous predicted data, the fourth stage of data presentation. Continuing, we show in figure 19, frequency correlation for $\theta_o = 0^\circ, 3^\circ$ and 6° for different parameter combinations. Though, for brevity, the other cases for different combinations of Ω, R and μ are omitted, those cases essentially depict the same trend as in Figure 19. The mode identification with the help of Floquet eigenvector analysis was found to be consistent with the constant coefficient approximation at low advance ratios ($\mu < 0.2$). In general ($0 \lesssim \mu \lesssim 0.55$), the term such as "lag regressing mode" implies the dominance of that particular mode, though coupled with other modes. It is good to reiterate that at high advance ratios the terms "regressing, collective and progressing" have less direct physical meaning than at low advance ratios.[4,10,11] No difficulties were experienced in mode identification. However, this experience should be tempered by the fact that the analytical model is relatively of small dimension (15x15 state matrix) with modest interblade coupling, and that for isolated rotors with rigid flap-lag blade the coupled rotating frequencies do not appreciably deviate from the corresponding uncoupled values.[10,11] Further, the blade-to-blade coupling is introduced only by dynamic inflow whose influence is expected to decrease with increasing blade pitch.[4,9] Yet, the frequency correlation in figure 19 is quite interesting in that it shows the necessity and viability of the Floquet eigenvector approach, particularly at high advance ratios.[4] We mention parenthetically that in an earlier analytical study,[4] the same approach of identifying modes was used for a coupled rotor-body system (29x29 state matrix) for which it was found that the coupled frequencies appreciably deviated from uncoupled frequencies with increasing advance ratios due to body dynamics.

Further, figure 19 shows that the overall frequency correlation for all the three cases ($\theta_o = 0^\circ$, 3° and 6°) is excellent, although the slight deviation between theory and data increases with increasing θ_o. For $\theta_o = 6^\circ$, it is interesting to compare the frequency correlation in figure 19c with the corresponding damping correlation in figure 16a. The frequency correlation is much better than the damping correlation. This is partly due to the fact that, compared to damping, the frequencies are less sensitive to modeling assumptions (e.g. uniform steady inflow vis-a-vis non-uniform steady inflow). The other reason, as noted earlier, seems to be peculiar to isolated rotors for which the coupled (rotating) frequencies are not substantially different from uncoupled frequencies,[11,12] in sharp contrast to rotor-body systems.[4] The measured coupled and uncoupled frequency data for the present isolated rotor model and references10,11,and 4 corroborate this other reason.

Figure 20 shows the damping correlation for $\theta_o=0^\circ$, $\Omega=1000$ and R=0 at advance ratios of 0.3 and 0.45. It is good to mention that for the data in figure 20, the inplane structural damping is slightly higher when compared to the data presented thus far (0.22% critical compared to 0.185%). The predicted data with and without dynamic inflow are respectively shown by full and dotted lines. As seen from figures 9, we should expect appreciable stall effects for $\alpha_s > 10^\circ$ for $\mu=0.3$. And,for $\mu=0.45$ the linear theory is practically invalid for $\alpha_s > 4^\circ$. A striking feature is that the predicted data (without inflow) which

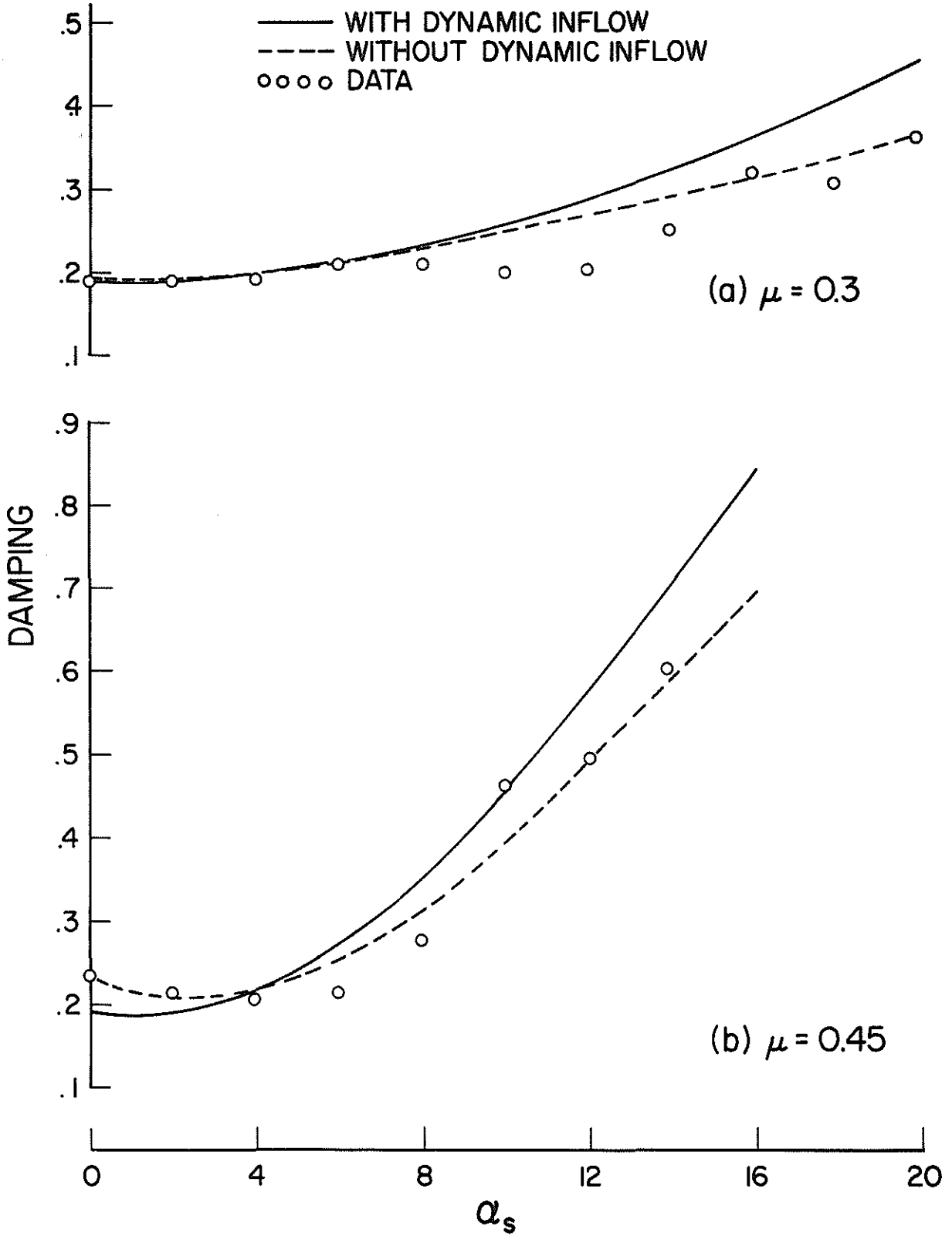

Fig. 20 LAG REGRESSING MODE DAMPING CORRELATIONS, IN SUBSTALL AND STALL (Ω=1000 RPM, R=0, θ_o= 0°)

also does not account for stall shows "better correlation." The predicted data without dynamic inflow are anomalous in stall conditions and lead to the erroneous conclusion that the inclusion of dynamic inflow degrades correlation. The fact is that the theory without and with dynamic inflow needs to be appropriately resolved for stall conditions. If blithely applied, such anomalous data may lead to incorrect conclusions. Thus, the correlation in figure 20 demonstrates the need to resolve the anomalous data for stall effects under the analytically demanding conditions of forward flight.

Before concluding the data presentation, we study the role of flap-lag parameter R. The data thus far presented for R=0 and R=1 lead to the finding that R is not an important parameter by *itself* in increasing the lag regressing mode damping. This finding is consistent with earlier experimental studies in hover on isolated blades and coupled rotor-body systems.[1,3,7]

6. CONCLUDING REMARKS

Thus far, we presented the correlation between theory and data (damping and frequency). *That* correlation, if not stated otherwise, refers to damping and leads to the following concluding remarks:

1. In hover, the theoretical predictions are in general agreement with the measured data. However, some discrepancies at high rotational speeds and blade pitch settings are perhaps associated with recirculation effects.

2. In Forward flight at θ_0=0°, the correlation between theory and data is superb in substall (per cent stall region <10). Discrepancies between theory and data are found to be at high $\mu\alpha_s$ values and can be reasonably identified with stall effects.

3. In forward flight at θ_0= 3°, the overall correlation is very good. However, for high values of shaft angles (α_s>12°), certain discrepancies are identified, as being associated with either nonuniform steady inflow, or with stall or with both.

4. In forward flight at θ_0= 6°, the theory, although not giving an accurate quantitative prediction in substall, is nevertheless qualitatively accurate. The discrepancies are not associated with stall. We expect that they are associated with nonuniform steady inflow. This expectation is based on the observation that the discrepancies are higher at very low advance ratios (μ=0.05 or 0.1) when compared to those at advance ratios close to 0.2.

5. The inclusion of dynamic inflow improves overall correlation, although for several cases in forward flight that improvement is at best, marginal.

6. In substall, for the shaft angles considered under untrim conditions, the theoretical prediction that the damping levels of the lag regressing mode increase with increasing μ is confirmed by data.

7. The flap-lag coupling parameter R by itself does not seem to be effective in increasing the damping level of the lag regressing mode.

8. Excellent frequency correlation between theory and data was observed throughout. However it is not a valid indication of the adequacy of the theory in predicting damping.

9. In stall conditions of forward flight, the linear theory without dynamic inflow gives results that often give the erroneous impression that the predicted data without dynamic inflow correlate better than the predicted data with dynamic inflow. This is due to the fact that such results are anomalous without being resolved for stall-effect corrections.

7. ACKNOWLEGEMENT

The authors would like to thank Mrs. Antonia Margetis and Mrs. Nancy Ward Anderson for their hard work and persistence in word processing this paper.

This work is sponsored by the NASA-Ames Research Center and administered under Grant NCC 2-361.

8. REFERENCES

1. Ormiston, R. A., " Investigations of Hingeless Rotor Stability", Vertica, Vol. 7, No. 2, 1983, pp. 143-181.

2. Friedmann, P. P., "Formulation and Solution of Rotary-Wing Aeroelastic Stability and Response Problems", Vertica, Vol. 7, No.2, pp.101-141, 1983.

3. Bousman, William G., "A Comparison of Theory and Experiment for Coupled Rotor-Body Stability of a Hingless Rotor" ITR Methodology Assessment Workshop, NASA Ames Research Center, Moffett Field, California, June 1983.

4. Nagabhushanam, J. and Gaonkar, G. H., "Rotorcraft Air Resonance in Forward Flight with Various Dynamic Inflow Models and Aeroelastic Couplings", Vertica, Vol.8, No. 4, December, 1984, pp. 373-394.

5. Gaonkar, G. H. and Peters, D. A., "A Review of Dynamic Inflow and Its Effect on Experimental Correlations" Proceedings of the Second Decennial Meeting on Rotorcraft Dynamics, AHS and NASA Ames Research Center, Moffett Field, California, November 7-9, 1984. Paper No. 13.

6. Neelakantan, G. R. and Gaonkar, G. H., "Feasibility of Simplifying Coupled Lag-Flap-Torsional Models For Rotor Blade Stability in Forward Flight", Tenth European Rotorcraft Forum, The Hague, The Netherlands, August 28-31, 1984, Paper No. 53 (To appear in Vertica, Vol. 9, No.3, 1985).

7. Bousman, W. G., Sharpe, D. L., and Ormiston,, R. A., "An Experimental Study of Techniques for Increasing the Lead-Lag Damping of Soft Inplane Hingeless Rotors", Proceedings of the American Helicopter Society 32nd Annual National Forum, Washington, D. C., May 1976, Preprint No. 730.

8. Ormiston, R. A. and Bousman, W. G., "A Study of Stall-Induced Flap-Lag

Instability of Hingeless Rotors", Preceedings of the American Helicopter Society 29th Annual National Forum, Washington, D. C., May 1973, Preprint No. 730.

9. Gaonkar, G. H. et al, "The Use of Actuator-Disc Dynamic Inflow for Helicopter Flap-Lag Stability", Journal of the American Helicopter Society, July 1983, Vol. 28, No. 3, pp 79-88.

10. Gaonkar, G. H., and Peters, D. A., "Use of Multiblade Coordinates for Helicopter Flap-Lag Stability with Dynamic Inflow," Journal of Aircraft, Vol. 17, No. 2, 1980, pp.112-118.

11. Peters, D. A., and Gaonkar, G. H., "Theoretical Flap-Lag Damping with Various Dynamic Inflow Models," Journal of the American Helicopter Society, July 1980, Vol. 25, No. 3, pp.29-36.

12. Gaonkar, G. H., Simha Prasad, D. S., and Sastry, D. S. "On Computing Floquet Transition Matrices of Rotorcraft", Journal of the American Helicopter Society, Vol. 26, No. 3, July 1981, pp. 56-62.

13. Nagabhushanam, J., Gaonkar, G. H., and Reddy, T.S.R., "Automatic Generation of Equations for Rotor-Body Systems with dynamic Inflow for A-Priori Ordering Schemes," Seventh European Rotorcraft Forum, Garmisch-Partenkirchen, Federal Republic of Germany, September 8-11, 1981, Paper No. 37

14. Nagabhushanam, J., Gaonkar, G. H., Srinivasan, P., and Reddy T.S.R., Users' Manual for Automatic Generation of Equations of Motion and Damping Levels for Some Problems of Rotorcraft Flight Dynamics, R & D Report, HAL-IISC Helicopter Programme, Indian Institute of Science, Bangalore, India, October 1984.

15. Bousman, W. G. , and Winkler, D. J.: "Application of the Moving-Block Analysis," Paper 81-0653-CP, 22nd Structures, Structural Dynamics, & Materials Conference, Atlanta, Ga., April 1981.